Hot wire chemical vapor deposition for silicon photonics: An emerging industrial application opportunity

A. Tarazona, T. Domínguez Bucio, S.Z. Oo, R. Petra, A.Z. Khokhar, Stuart A. Boden, F.Y. Gardes, G.T. Reed, H.M.H. Chong

PII: S0040-6090(19)30134-8
DOI: https://doi.org/10.1016/j.tsf.2019.02.048
Reference: TSF 37185

To appear in: *Thin Solid Films*

Received date: 1 November 2018
Revised date: 27 February 2019
Accepted date: 27 February 2019

Please cite this article as: A. Tarazona, T.D. Bucio, S.Z. Oo, et al., Hot wire chemical vapor deposition for silicon photonics: An emerging industrial application opportunity, Thin Solid Films, https://doi.org/10.1016/j.tsf.2019.02.048

Hot Wire Chemical Vapor Deposition for Silicon Photonics: An emerging Industrial Application Opportunity

A. Tarazona*[a], T. Domínguez Bucio[a], S. Z. Oo[a,b], R. Petra[b], A. Z. Khokhar[b], Stuart A. Boden[b], F. Y. Gardes[b], G. T. Reed[a], and H. M. H. Chong[b]

a. Optoelectronics Research Centre, University of Southampton, Highfield, Southampton, SO17 1BJ, U. K.
b. School of Electronics and Computer Science, University of Southampton, Highfield, Southampton, SO17 1BJ, U. K.

*****Corresponding Author: Dr Antulio Tarazona, e-mail: A.Tarazona@soton.ac.uk, Telephone: +44 238059 9104, fax: +44 238059 3029

Abstract

In this work different silicon photonic devices, including straight waveguides, multi-mode interference devices and Mach-Zehnder interferometers, were fabricated and characterized on hot-wire chemical vapor deposition (HWCVD) silicon nitride (SiN) layers deposited at temperatures below 350 ^{o}C. These layers presented a hydrogen concentration of 13.1 %, which is lower than that achieved with plasma enhanced chemical vapor deposition at these deposition temperatures. The lowest reported optical propagation losses of 6.1 dB/cm and 5.7 dB/cm, 1550 nm and 1310 respectively, for straight SiN waveguides prepared by HWCVD was measured. We demonstrated that silicon nitride SiN, prepared using HWCVD, is a viable material for silicon photonics fabrication.

Keywords: Silicon Photonics, Hot wire Chemical Vapor Deposition, Silicon Nitride, Mach-Zehnder Interformeter, Multimode Interferometer, silicon photonics waveguides

Introduction

Silicon Photonics has become a game changer as the next generation optical data communication devices for short-range interconnects and signal processing due to its advantage over the conventional electrical alternative, to low power consumption, low cost and most importantly, complementary metal-oxide-semiconductor (CMOS) compatibility [1][2]. So far, silicon photonics is based on low loss crystalline silicon on insulator to form the optical circuits. However, there is an increasing interest for amorphous silicon (a-Si:H) [3] and silicon nitride (SiN) [4] as part of the photonic integrated circuit because of its low propagation losses and implementation costs. Low temperature has also caught the attention of the academic and industrial world to integrate silicon photonic devices on top of CMOS at the back-end-of-the-line and multilayer silicon photonic devices, where the temperature needs to be below 400^{o}C for the complete fabrication of the optical components [5]. Mao et al. reported plasma enhanced chemical vapor deposition (PECVD) SiN waveguides fabricated at 400 ^{o}C with a propagation loss of 2.1 dB/cm after reduction of hydrogen content in the film layer [6].

There has been a recent increase in hot-wire chemical vapor deposition (HWCVD) publications and interest in a-Si:H, doped Si and SiN and its principles are relatively simple [7]. HWCVD was chosen as it exhibits different advantages over PECVD for different applications [8][9]. In particular, the low-temperature deposition of SiN [10] for silicon photonic waveguides have been demonstrated using HWCVD. HWCVD not only enables low-temperature processing but also allows to deposit SiN [11] layers with low hydrogen concentration respect to their PECVD.

In this work, HWCVD was chosen as the means to deposit SiN with low hydrogen concentration and to demonstrate the viability of HWCVD SiN, we demonstrate the optical characteristics of straight waveguides, multimode interferometer (MMI) and Mach-Zehnder interferometer (MZI) devices. In this report working silicon photonic devices beyond straight waveguides using HWCVD are presented and discussed to highlight the suitability of HWCVD in the fabrication of silicon photonics components and circuits.

Experimental details

The SiN layers with a refractive index close to 2.0 were grown using the Echerkon Nitor 301 system, described in a previous publication [12]. These layers were deposited at 350 ^{o}C on SiO_2 layers previously formed on a 6" p-type Si. The SiN layers were deposited using a NH_3 to SiH_4 ratio of 16 with a pressure of 6.5 Pa. The filament temperature was kept at 1850 ^{o}C.

Afterward, electron beam lithography was used to define the optical devices and the grating couplers, which were transferred to the SiN layers using standard inductive coupled plasma etching with a chemistry containing SF_6 and CHF_3. A 1 μm thick SiO_2 cladding was deposited using PECVD to cover the devices. Figure 1 depicts the schematic cross-section of the SiN core, SiO_2 cladding and Buried Oxide (BOX) on the Si substrate.

The physical and optical properties of the obtained layers were characterized. Ellipsometry (Woolham M-2000 spectroscopic ellipsometer) was used to determine the thickness and refractive index of the layers. A Focused Ion Beam (FIB) system equipped with Field Emission Scanning Electron Microscope (FIB-FESEM Zeiss NVision 40) was employed to inspect the morphology of the films. A cross-section of the waveguide was cut and polished using a 30 kV Ga FIB beam with beam currents ranging from 13 nA to 80 pA. The imaging of the cross-sectional surface was carried out at a tilt angle of 54 degrees and a working distance of 5 mm, with an SEM accelerating voltage of 2 kV and an in-lens detector. Finally, Fourier Transform Infrared Spectrometry (FTIR) was performed in the range between 400 and 6000 cm-1 with a resolution of 0.96 cm-1 using a Varian 600 FTIR spectrometer to ascertain the hydrogen concentration of the films.

The bond concentrations of the SiN layers were extracted from the FTIR spectra following the method described in detail by Yin at al. [13] using the proportionality factors K[N-H] = $8.2\text{x}10^{16}$ cm^{-1}, K[Si-H] = $5.9\text{x}10^{16}$ cm^{-1} and K[Si-N] = $2.4\text{x}10^{16}$ cm^{-1}. The atom concentrations corresponding to hydrogen ([H]), nitrogen ([N]) and silicon ([Si]) where then estimated from the FTIR bond concentrations using equations 1 to 3 [13,14]:

$$[H] = [N-H] + [Si-H] \quad (1)$$

$$[N] = \frac{[Si-N] + [N-H]}{3} \quad (2)$$

$$[Si] = \frac{[Si-N] + [Si-H]}{4} \quad (3)$$

Where [N-H] is the concentration of the N-H bonds, [Si-H] the concentration of Si-H bonds and [Si-N] the concentration of Si-N bonds incorporated in the films. In a similar manner, the hydrogen concentration in atomic percentage and the N/Si ratio of the films were approximated from the calculated atom concentrations. It is important to mention that the values obtained for the hydrogen concentration and the N/Si ratio are approximations that underestimate the amount of Si atoms present in the films as equation 3 dismisses the contribution of the Si-Si bonds that form in films with N/Si<1.33. Under this context, the

hydrogen content and the N/Si ratio of films with a high silicon content will be overestimated using these equations. However, as the films studied in this work have a composition close to stoichiometry, it is assumed that the presence of Si-Si atoms is negligible and, so, the approximations provide a good estimate of the actual values. More accurate values for the N/Si ratio of the films can be obtained using alternative characterization techniques such as elastic recoil detection and Rutherford back scattering [14].

The propagation losses of the studied materials were measured at 1550 nm wavelength using the cutback method with waveguides of different length, a schematic diagram of the measurement set-up is depicted in Figure 2.

Theory/calculation

The dimensions of the SiN waveguides used in this study were selected to be 300 nm for the thickness and 1200 nm for the width to ensure single-mode propagation based on a detailed analysis of the guided modes performed using the commercial software MODE Solutions. Following a similar approach, the width (W_{MMI}) and length (L_{MMI}) required to achieve a 3 dB splitting ratio between the output ports of 1x2 MMI devices were calculated using eigenmode expansion simulations in MODE Solutions. In this case, the simulation results suggested that a length of 65 μm and a width of 11 μm were adequate to achieve the required splitting ratio using an output spacing equal to $W_{MMI}/2$. In addition, the width of the input/output tapers of the MMI was optimized to 5 μm and their length to 20 μm in order provide the lowest optical loss possible. Using these optimized dimensions, the minimum MMI loss predicted for transverse electric polarization was of 0.1 dB. Figure 4a shows the field profile obtained using the optimized dimensions for the 1x2 MMI devices. The 1x2 MMI devices were finally used to fabricate 1x1 MZI devices with optical path length differences ranging between 10 and 100 um that can be used as wavelength filters for a wide variety of photonic applications.

Results and Discussion

Figure 3a and 3b show the extracted insertion losses of the transverse electric fundamental mode within the HWCVD SiN waveguides at 1310 nm and 1550 nm as a function of varying lengths ranging between 0.05 and 1.7 cm. The linear regressions fitted to these points result in a propagation loss of 5.7dB/cm at 1310 nm and 6.1dB/cm at 1550nm. The optical propagation losses obtained in this work at 1550nm are higher than the losses ~3dB/cm observed in waveguides fabricated on PECVD SiN [1]. Amongst the factors contributing to the propagation losses of SiN films prepared at temperatures below 400^{o}C are the absorption

losses due to their hydrogen content and the scattering losses produced by their morphology. FTIR was employed to gain an insight into the SiN material composition.

Figure 4a shows the FTIR spectrum covering the range between 400 and 5000 cm^{-1} that was acquired to analyse the Si-N, Si-H and N-H bands located at around 860, 2200 and 3330 cm^{-1}, respectively. The silicon ($26.8x10^{21}$ cm^{-3}), nitrogen ($37.3x10^{21}$ cm^{-3}) and hydrogen ($9.6x10^{21}$ cm^{-3}) atomic concentrations of the studied film were calculated using the bond concentrations extracted from the FTIR spectrum, also shown in figure 4a, following the procedure outlined in the experimental details. It can be seen that the N/Si value estimated with the calculated atomic concentrations is close to the stoichiometric ratio of 1.33 and that the hydrogen concentration at 13.1%, which is responsible for absorption losses, is lower than typical values reported for PECVD at above 20%. The lower hydrogen concentration suggests that the SiN devices prepared using HWCVD should exhibit lower propagation losses due to the reduced absorption losses of the films compared to those prepared using PECVD at similar temperatures, as indicated in the detailed study of the H concentration and deposition condition of PECVD layers published by Dominguez et al. [17]. Therefore, the morphology of the material should be having a significant contribution to the propagation losses of the waveguides. In fact, contrary to the higher losses observed at 1550nm in both HWCVD and PECVD layers when the contribution of absorption losses is significant, the optical losses observed at both 1310nm and 1550nm are comparable. This closeness strongly suggests that the propagation losses of the studied HWCVD layers is limited by the scattering losses produced by the structure of the material layer. FIB-FESEM images were acquired to gain an insight into the film morphology. Figure 4b shows a FIB-FESEM image of the SiN core embedded in SiO_2, the inset highlights some voids observed throughout the SiN core, the voids are magnified and highlight in the inset of the FIB-SEM image. It can be observed that the SiN as well as the SiO_2 exhibit amorphous structures without any underlying pattern. However, the voids observed on the cross section are likely to be distributed all along the SiN providing light scattering centers which would significantly contribute to the light propagation losses. Hence, if these voids are eliminated from morphological structure an improvement of the overall propagation losses should be achieved.

Figure 5b depicts a microscope image of the fabricated 1x2 SiN MMI devices, while figure 6a shows a microscope image of the 1x2 SiN MMI devices cascade in series in order to determine the propagation loss per MMI. The losses observed in each increasing chain were fitted to a linear trend as illustrated in figure 6b. The losses per MMI were estimated to be close to 5.2 dB. This value is higher than the minimum losses of less than 1 dB per MMI

output obtained with simulations, and higher than values observed in MMIs fabricated on PECVD SiN layers. Similar to what happened with the optical losses of the straight waveguides, which suggests that the increased losses observed in the MMI devices are the result of the relatively high optical propagation losses of the material not only due to the geometry of the devices but to the hydrogen content and the morphology of the SiN films. Additional losses could have also arisen from the sidewall roughness present in the devices due to the etching process.

An example of the spectra measured for MZI devices with different optical path length is illustrated in figure 7a, a microscope image of MZI devices with different arm length, 100 µm and 700 µm, were fabricated with SiN layers embbeded in SiO_2. The free-spectral range (FSR) of each MZI, which corresponds to the spacing between two successive transmission maxima, can be estimated from the measured spectra. In this case, it was observed that MZI devices with an optical path length difference of 100 µm results in a FSR of around 15 nm, whereas an optical path length difference of 700 µm results in a FSR of 7 nm. These observations provide a starting point for the design of MZI with different FSR for a variety of photonic applications in the NIR.

Conclusions

The low-temperature deposition of SiNx below 400 ^{o}C using HWCVD has produced optical waveguides of 6.1 dB/cm loss at 1550 nm wavelength. MMI and MZI waveguide devices have shown to have a similar response compared to that observed in devices fabricated on PECVD SiN. Although the HWCVD devices exhibit insertion losses that are 4 dB higher than those achieved with PECVD SiN due to the increased optical losses of the material, the demonstrated devices have the potential for silicon photonics integrated circuits in data communication, bio/environmental sensing applications. In this work, silicon photonic devices prepared using HWCVD SiN has shown the potential for the fabrication of the most widely used elements of Photonic integrated circuits. The HWCVD SiN lower hydrogen concentration has an advantage and partially compensate the propagation losses produced by voids and other morphological defects. The morphological defects of the SiN core have been identified as a possible source for the propagation losses and future work would concentrate on addressing this.

Acknowledgment: This work was supported by the Engineering and Physical Sciences Research Council (EPSRC) Grants EP/L00044X/1 and EP/N013247/1. The authors would

like to thank Southampton Nano Fabrication Centre, University of Southampton. Reed is a Royal Society Wolfson Merit Award holder. He is grateful to both the Royal Society and the Wolfson Foundation. One of the authors, R. Petra, would like to acknowledge the University of Technology Brunei Ph.D. scholarship scheme.

References

[1] R. Soref, The Past, Present, and Future of Silicon Photonics, IEEE J. Sel. Top. Quantum Electron. 12 (2006) 1678–1687. doi:10.1109/JSTQE.2006.883151.

[2] M. Asghari, A. V. Krishnamoorthy, Energy-efficient communication, Nat. Photonics. 5 (2011) 268–270. doi:10.1038/nphoton.2011.68.

[3] G. Cocorullo, F.G. Della Corte, R. De Rosa, I. Rendina, A. Rubino, E. Terzini, Amorphous Silicon Waveguides and Interferometers for Low-Cost Silicon Optoelectronics, SPIE 3278, Integr. Opt. Devices II. 3278 (1998) 286–292. doi:10.1117/12.298212.

[4] A.Z. Subramanian, P. Neutens, A. Dhakal, R. Jansen, T. Claes, X. Rottenberg, F. Peyskens, S. Selvaraja, P. Helin, B. DuBois, K. Leyssens, S. Severi, P. Deshpande, R. Baets, P. Van Dorpe, Low-Loss Singlemode PECVD Silicon Nitride Photonic Wire Waveguides for 532–900 nm Wavelength Window Fabricated Within a CMOS Pilot Line, IEEE Photonics J. 5 (2013) 2202809–2202809. doi:10.1109/JPHOT.2013.2292698.

[5] S. Zhu, G.Q. Lo, D.L. Kwong, Low-loss amorphous silicon wire waveguide for integrated photonics: effect of fabrication process and the thermal stability, Opt. Express. 18 (2010) 25283. doi:10.1364/OE.18.025283.

[6] S.C. Mao, S.H. Tao, Y.L. Xu, X.W. Sun, M.B. Yu, G.Q. Lo, D.L. Kwong, Low propagation loss SiN optical waveguide prepared by optimal low-hydrogen module, Opt. Express. 16 (2008) 20809. doi:10.1364/OE.16.020809.

[7] H. Matsumura, Formation of silicon-based thin films prepared by Catalytic Chemical Vapor Deposition (Cat-CVD) method, Japanese J. Appl. Physics, Part 1 Regul. Pap. Short Notes Rev. Pap. 37 (1998) 3175–3187.

[8] S. Nishizaki, K. Ohdaira, H. Matsumura, Comparison of a-Si TFTs fabricated by Cat-CVD and PECVD methods, Thin Solid Films. 517 (2009) 3581–3583. doi:10.1016/j.tsf.2009.01.026.

[9] V. Verlaan, R. Bakker, C.H.M. van der Werf, Z.S. Houweling, Y. Mai, J.K. Rath, R.E.I. Schropp, High-density silicon nitride deposited at low substrate temperature with high deposition rate using hot wire chemical vapour deposition, Surf. Coatings Technol. 201 (2007) 9285–9288. doi:10.1016/j.surfcoat.2007.03.057.

[10] T. Domínguez Bucio, A. Tarazona, A.Z. Khokhar, G.Z. Mashanovich, F.Y. Gardes, Low temperature silicon nitride waveguides for multilayer platforms, in: L. Vivien, L. Pavesi, S. Pelli (Eds.), Proc. SPIE 9891, Silicon Photonic Integrated Circuits V, 2016 98911T. doi:10.1117/12.2227590.

[11] F. Ay, A. Aydinli, Comparative investigation of hydrogen bonding in silicon based PECVD grown dielectrics for optical waveguides, Opt. Mater. (Amst). 26 (2004) 33–46. doi:10.1016/j.optmat.2003.12.004.

[12] M.T. de Leon, A. Tarazona, H. Chong, M. Kraft, Design, Modeling, Fabrication, and

Evaluation of Thermoelectric Generators with Hot-Wire Chemical Vapor Deposited Polysilicon as Thermoelement Material, J. Electron. Mater. 43 (2014) 4070–4081. doi:10.1007/s11664-014-3352-6.

[13] Z. Yin, F.W. Smith, Optical dielectric function and infrared absoprtion of hydrogenated amorphous silcon nitride films: Experimental results and effective-medium-approximation analysis, Phys. Rev. B. 42 (1990) 3666–3672. doi:10.1103/PhysRevB.42.3666.E.

[14] Bustarret, M. Bensouda, M.C. Habrard, J.C. Bruyère, S. Poulin, S.C. Gujrathi, Configurational statistics in a - Si x N y H z alloys: A quantitative bonding analysis, Phys. Rev. B. 38 (1988) 8171–8184. doi:10.1103/PhysRevB.38.8171.

[15] N. Sherwood-Droz and M. Lipson, Scalable 3D dense integration of photonics on bulk silicon, Opt.Express 19 (2011) 17758. doi: 10.1364/OE.19.017758

[16] T. Domínguez Bucio, A. Tarazona, A.Z. Khokhar, G.Z. Mashanovicha, F.Y. Gardes, Hot-wire chemical vapour deposition for silicon nitride waveguides, ECS Trans.72 (2016) 269-272. doi:10.1149/07204.0269ecst.

Figures

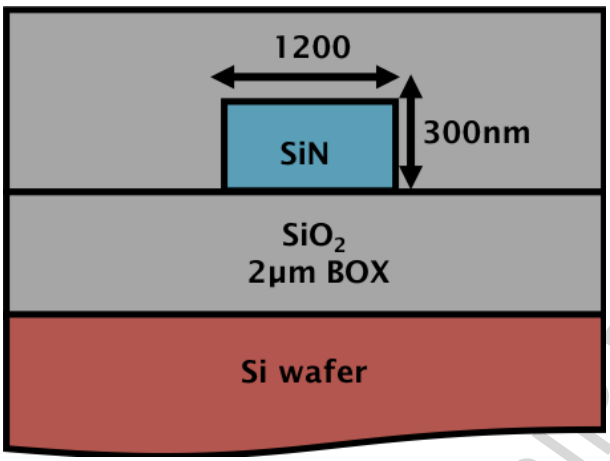

Figure 1 Schematic cross-section diagram of the SiN silicon photonic devices indicating the dimensions of the core, the cladding, and BOX on a Si wafer.

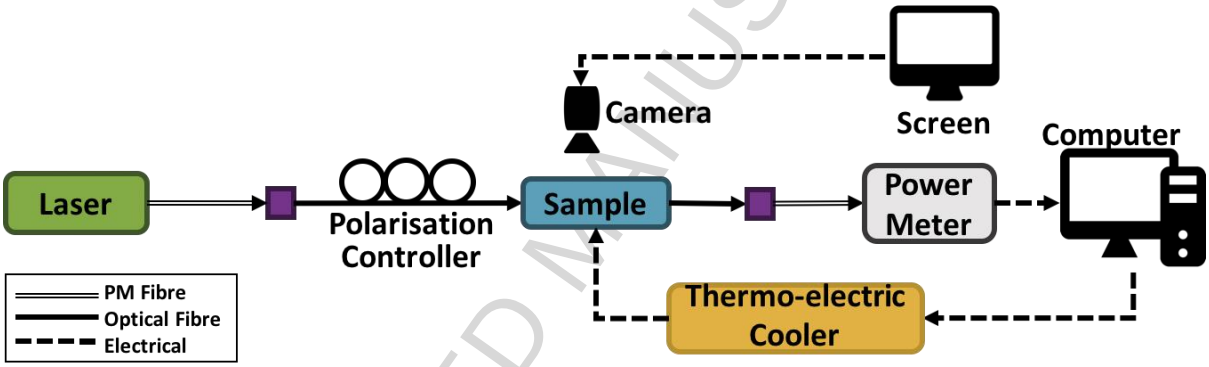

Figure 2 Schematic diagram of the instrumental set up to measure the optical performance of silicon photonic devices.

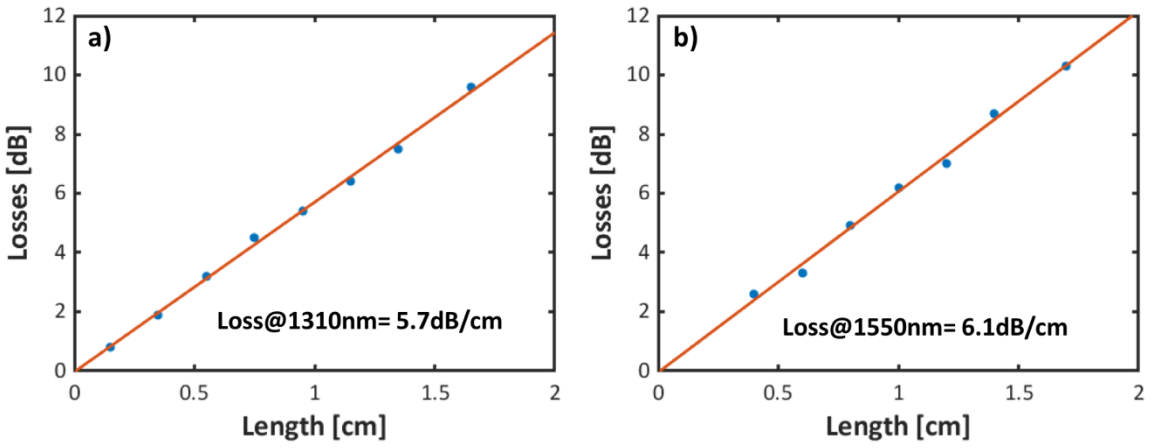

Figure 3 a) Measured propagation loss as a function of the length for SiN waveguides at 1310 nm wavelength b) Measured propagation loss as a function of the length for SiN waveguides at 1550 nm wavelength.

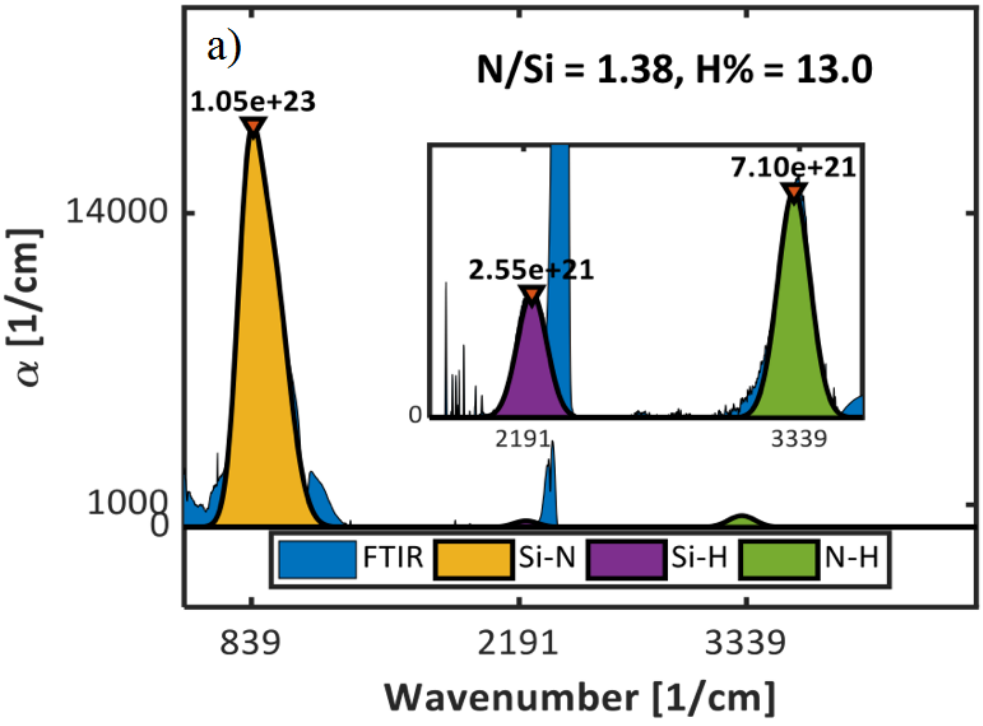

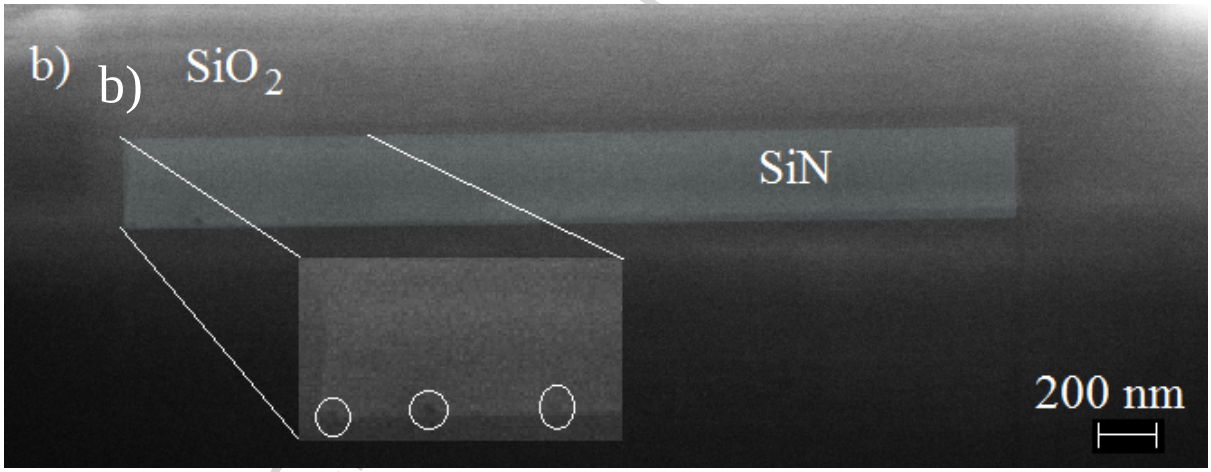

Figure 4 a) FTIR spectrum of the HWCVD SiN film. The inset shows an expanded view of the 3500 to 2000 cm^{-1} region, corresponding to the bands for Si-H at 2200 cm^{-1} and N-H at 3300 cm^{-1}. The calculation results of the N to Si ratio and hydrogen concentration are shown at the top-right corner. b) FIB-FESEM images of the cross-section of the SiN waveguide, light green, embedded in SiO_2, inset highlights with circle voids present in the SiN core.

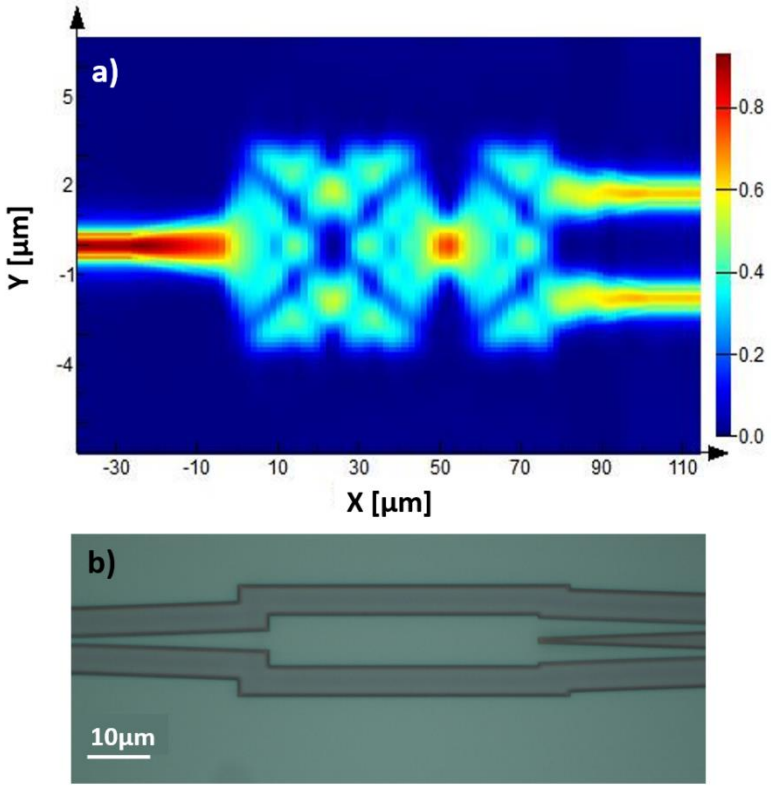

Figure 5 a) Intensity profile obtained with the eigenmode solver of MODE solutions for the 1x2MMI with optimized dimensions b) Microscope image of a SiN MMI fabricated using the results from the FDTD as guidance for the dimensions.

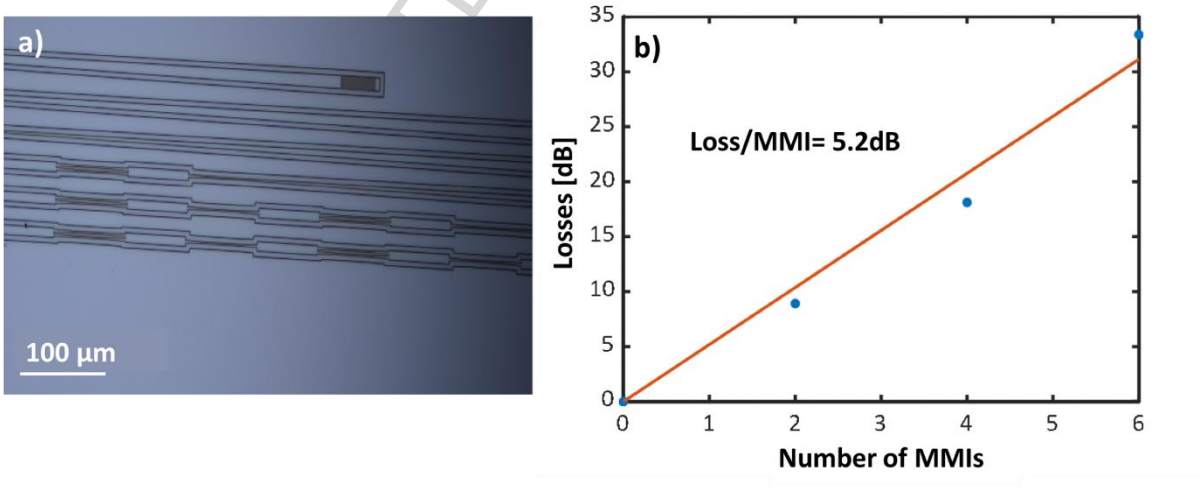

Figure 6 a) Microscope image of SiN MMIs cascaded in series to determine the propagation losses per number of MMI. b) Optical losses as function of the number of MMIs.

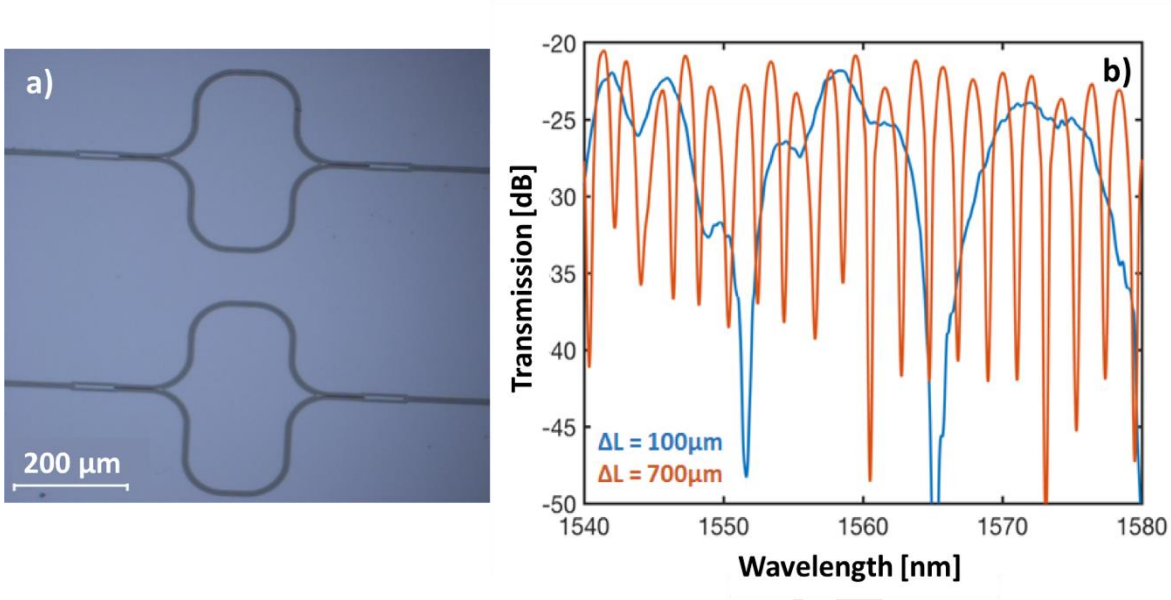

Figure 7 a) Microscope image of MZI devices with different arm length fabricated with SiN, b) MZI spectral response around the C-band of the telecommunication spectrum for 2 different arm lengths, blue 100 µm and red 700 µm.

Highlights:

- Silicon nitride (SiN) films were prepared by Hot Wire Chemical Vapor Deposition.
- Their morphology and H_2 were assessed to elucidate sources of propagation losses.
- Propagation losses of 6.1 dB/cm were measured on the HWCVD SiN waveguides.
- Multimode interferometers with propagation losses of 5.2 dB were fabricated.
- Built Mach-Zehnder interferometers showed free-spectral ranges of 7 and 15nm.